

Terahertz detectors based on all-dielectric photoconductive metasurfaces

Oleg Mitrofanov,^{a,b,*} Thomas Siday,^a Polina P. Vabishchevich,^{b,c} Lucy Hale,^a
Charles Thomas Harris,^{b,c} Ting Shan Luk,^{b,c} John L. Reno,^{b,c} Igal Brener,^{b,c}

^a University College London, Electronic and Electrical Engineering Department,
Torrington Place, London, UK WC1E 7JE;

^b Center for Integrated Nanotechnologies, Sandia National Laboratories,
Albuquerque, NM, USA 87123;

^c Sandia National Laboratories, Albuquerque, NM, USA 87185.

ABSTRACT

Performance of terahertz (THz) photoconductive devices, including detectors and emitters, has been improved recently by means of plasmonic nanoantennae and gratings. However, plasmonic nanostructures introduce Ohmic losses, which limit gains in device performance. In this presentation, we discuss an alternative approach, which eliminates the problem of Ohmic losses. We use all-dielectric photoconductive metasurfaces as the active region in THz switches to improve their efficiency. In particular, we discuss two approaches to realize perfect optical absorption in a thin photoconductive layer without introducing metallic elements. In addition to providing perfect optical absorption, the photoconductive channel based on all-dielectric metasurface allows us to engineer desired electrical properties, specifically, fast and efficient conductivity switching with very high contrast. This approach thus promises a new generation of sensitive and efficient THz photoconductive detectors. Here we demonstrate and discuss performance of two practical THz photoconductive detectors with integrated all-dielectric metasurfaces.

Keywords: terahertz, perfect absorption, metasurface, photoconductive detector, magnetic dipole mode, Mie resonance, time-domain spectroscopy, plasmonic nanoantenna.

1. INTRODUCTION

Research on terahertz (THz) photoconductive (PC) devices has seen new developments in the last several years.^{1,2} The interest is driven by new insights in the underlying physics, advances in photonics, which allowed engineering remarkable properties by means of plasmonic and dielectric nanostructures, as well as noticeable improvements in performance of THz PC devices.¹⁻²

For THz PC detectors and emitters in particular, plasmonic nanostructures were used to enhance optical absorption in the PC region.³⁻⁷ It has led to more efficient devices with record THz emission powers⁴⁻⁶ and more sensitive detectors.^{3,7} However, plasmonic elements within the PC device architecture also result in partial absorption of the incident photons within the metal.⁸ These losses can be substantial, up to ~50% of incident photons. Furthermore, plasmonic elements introduced in contact with the PC channel may reduce the OFF-state resistivity of the PC device, and thus negatively affect performance of THz detectors, which require a high ON/OFF contrast. Therefore, PC devices, and particularly THz detectors, may benefit from alternative methods, which realize the benefits of plasmonic nanostructures without introducing their drawbacks.

The functionalities enabled by the plasmonic structures, and particularly enhanced absorption of incident photons, can also be realized with all-dielectric metasurfaces. In this contribution, we will discuss PC devices with the PC channel nanostructured as all-dielectric metasurfaces.

*o.mitrofanov@ucl.ac.uk

1.1 Photoconductive switch operation

The key process for operation for THz PC detectors is ultrafast switching of electrical conductivity under photon illumination between a highly resistive (OFF) and highly conductive (ON) state. We first review the process of photoexcitation of the PC switch in order to emphasize optimal optical and electronic properties for its operation. A schematic diagram of this process is shown in Figure 1. Incident photons generate electron-hole pairs in the structure; the charge carriers drift in the presence of electric field from a THz wave and produce a photocurrent proportionally to the electric field amplitude.

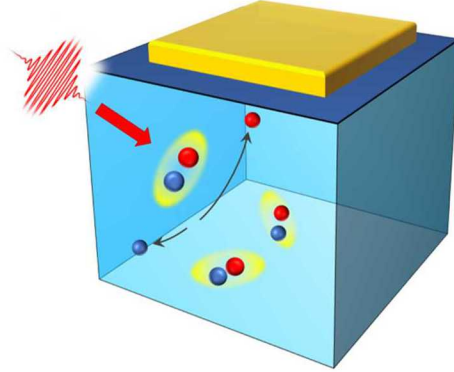


Figure 1. Schematic diagram of photoexcitation within the PC switch.

The switching times, typically in the sub-picosecond range, determine the detection bandwidth of PC THz detectors.⁹ For efficient operation of the detector, the charge carriers must be generated for the duration shorter than half-cycle of the THz wave. This is achieved by using ~100 fs optical pulses for photoexcitation, and specially designed ultrafast materials with sub-picosecond carrier lifetime. Among most commonly used ultrafast photoconductors is low-temperature grown (LT) GaAs, where sub-picosecond charge carrier lifetime is achieved through incorporation of charge trapping centers during the material growth and post-growth annealing.⁹

The combination of the 100 fs pulse excitation and the short carrier lifetime in LT GaAs therefore enables sub-picosecond switching times required for THz wave detection. However, the photogenerated electron-hole pairs drift only small distances during that time, and the vast majority of carriers are captured on trap centers within the PC channel before they can reach metallic contacts. This fundamentally limits the efficiency of THz PC detectors: although materials like LT GaAs allow achieving very high conductivity contrast on sub-picosecond time scale, the conversion efficiency (the number of carriers generated per incident photon) has been very low.

1.2 Efficient photoconductive switch architecture requirements

We can summarize three requirements for an efficient PC THz detector architecture as follows: (1) sub-picosecond recombination time for photo-excited charge carriers in the PC channel; (2) a high contrast in electrical conductivity for the ON and OFF states; and (3) efficient conversion of photons to charge carriers.

To improve the conversion efficiency without modifying the switching times or reducing the conductivity contrast, we explore the concept of all-dielectric metasurface, and aim to enhance optical absorption and to localize photon absorption only within a thin PC layer, significantly thinner than the absorption length in the material. For LT GaAs, which enables sub-picosecond switching time and very high switching contrast, the absorption length is ~1000 nm, about one order of magnitude longer than a typical charge drift length. Therefore, the main challenge is to localize and enhance absorption in an optically thin layer of LT GaAs.

2. PERFECT OPTICAL ABSORPTION IN ALL-DIELECTRIC METASURFACES

One of the remarkable functionalities that can be realized with metasurfaces is perfect absorption of light for selected wavelengths. It can be achieved even with a weakly absorbing layer of small thickness, much smaller than the absorption length. Perfect absorbers typically contain a metallic back reflector behind the absorbing layer. The reflector prevents propagation in the forward direction and also allows to create the condition of destructive interference for the reflected waves, such that the structure exhibits zero reflection at the selected wavelength and no transmission, i.e. the incident wave is fully absorbed by the metasurface.

However, the metallic reflector would also block THz waves, and therefore such an architecture would not work for THz detectors. The function of the metallic reflector can be also realized by an all-dielectric Distributed Bragg Reflector (DBR). This design is shown in Figure 3(a).

To achieve perfect absorption in this approach, we control reflectivity of the top surface by introducing an array of resonant nanoscale beams (nanobeams). This structure supports a mode similar in spatial distribution to the magnetic dipole mode of a cube. We design a nanobeam structure for LT GaAs with 5 period AlGaAs/GaAs DBR. The design is schematically illustrated in Figure 3(c). Details of this design can be found in Ref. 10, here we only summarize the main parameters: the LT GaAs nanobeam width and height are 90 and 70 nm respectively, the nanobeams are etched in a 160 nm thick layer of LT GaAs with a period of 280 nm. Using numerical simulations, we find that this structure can absorb >80% of incident light at 800 nm. However, there are also practical drawbacks of this design. The DBR in our design far from a good reflector, it has only 5 DBR periods and it contains GaAs as one of the DBR layers (due to material growth limitations). As a result, absorption and transmission occur in the DBR, limiting improvements in the device efficiency.

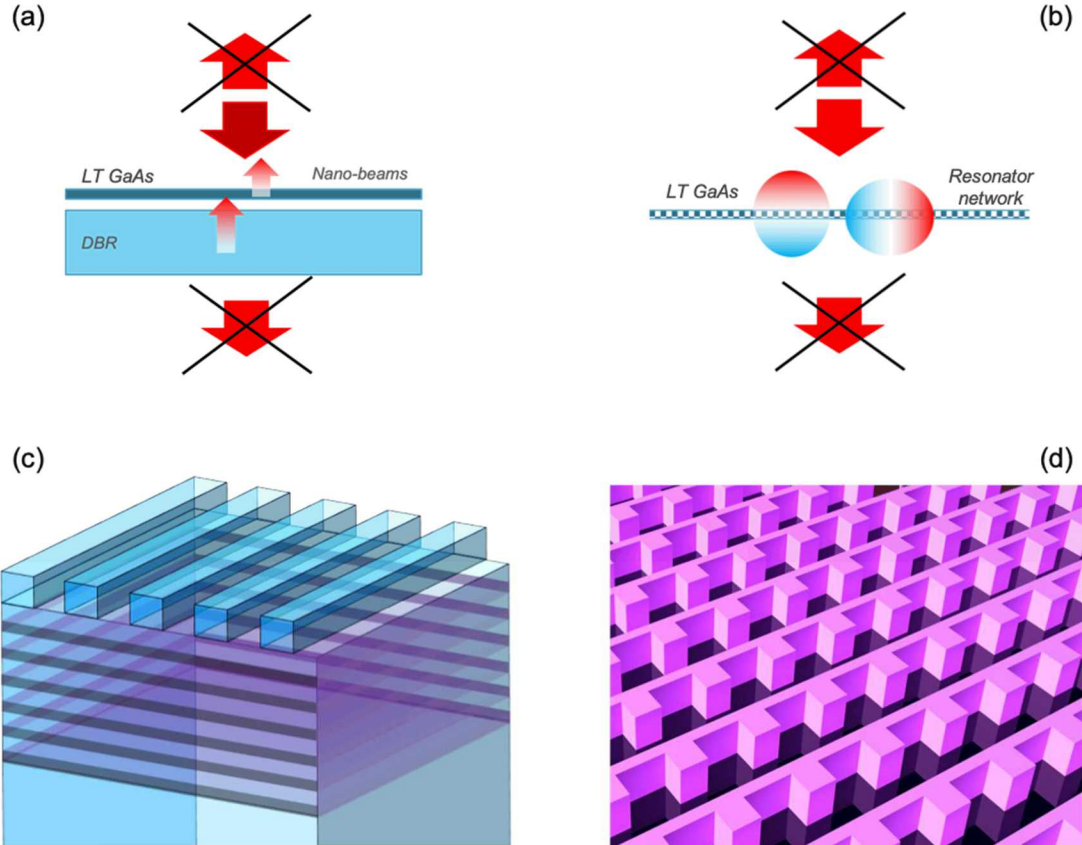


Figure 2. Two approaches for realizing perfect absorption using all-dielectric metasurfaces: (a) nanostructured thin LT GaAs layer with a DBR, and (b) network of resonators supporting two degenerate and critically coupled modes of opposite symmetry. (c, d) rendering of the corresponding nanostructures in the two approaches.

The second approach to achieve perfect absorption was proposed only recently,¹¹⁻¹³ and it is schematically illustrated in Figure 2(b). A metasurface can absorb all of the incident photons, if they couple to two degenerate modes of opposite symmetry, odd and even with respect to the metasurface plane, provided that the coupling for the two modes is critical. To realize this concept, we design an optical resonator supporting modes of odd and even symmetry at the laser excitation wavelength.

Our design is based on a cubic resonator. A cube supports a set of resonant Mie modes, with the lowest frequency mode being the magnetic dipole (MD) mode. There are three degenerate MD modes, and we will refer to these modes using the dominant component of the magnetic dipole vector M . Two of the modes have their dipole moments, M_x and M_y , in the xy -plane; the corresponding electric field distributions are odd with respect to the metasurface plane; the dipole moment of the third mode M_z is orthogonal to the plane, and the corresponding electric field distribution is even with respect to the plane.

Although the cubic resonator supports MD modes of both symmetries, the MD mode M_z is dark, i.e. it does not couple to a plane wave with the k -vector normal to the xy -plane. Only the modes with odd symmetry, M_x and M_y , are directly excited by this plane wave, and therefore perfect absorption using only MD modes in cubic dielectric resonators is impossible. However, we find that the MD mode M_z does get excited by light at normal incidence in resonator where the cubic symmetry is broken. We design a structure shown in Figure 2(d), which contains an array of cubes connected by beams aligned along one side of the cubes. We find that under normal excitation with linearly polarized light, E_y , two magnetic dipole modes, M_x and M_z , are excited in the structure. After optimizing geometrical parameters of the array numerically, we find that this structure enables perfect absorption in LT GaAs at 800 nm. Details of the resonator design and its effect on absorption properties can be found in Ref. 14.

3. TERAHERTZ DETECTORS WITH INTEGRATED METASURFACES

3.1 Integration of metasurfaces into the PC detector structure

We integrate the two designs for perfectly absorbing metasurfaces into the PC gap of the THz antenna detectors, as shown in Figure 3.

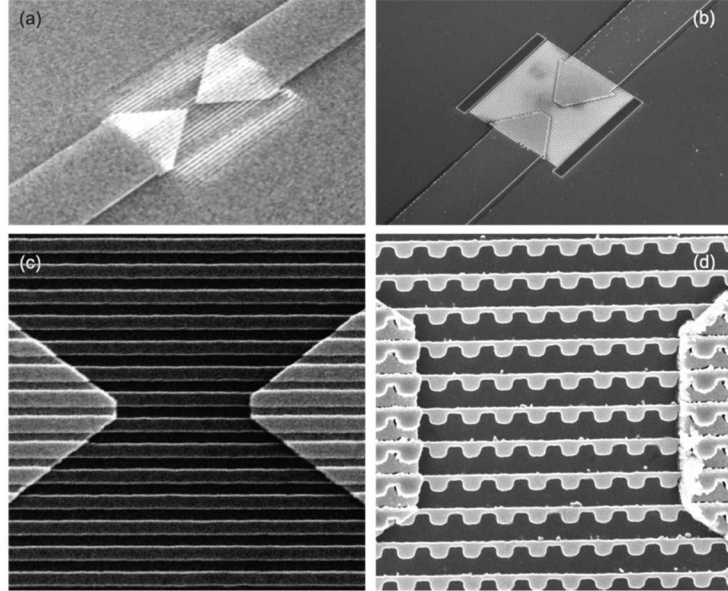


Figure 3. Scanning electron micrographs of PC THz detector antennae with integrated metasurfaces: (a) – metasurface with nanobeams and DBR, (b) – metasurface with a network of connected cubic resonators. Enlarged images of the corresponding photoconductive channels; (c) – the nanobeam metasurface detector with the PC gap of 1.5 μm ; (d) – the cubic resonator network metasurface with the PC gap of 3 μm .

A $20 \times 20 \mu\text{m}^2$ nanostructured region is patterned directly on the surface of LT GaAs and then antenna electrodes are deposited on top of the metasurfaces. Enlarged scanning electron images of the metasurface structures are shown in Figure 3(c,d). The structures are then bonded to sapphire substrates with epoxy and the original GaAs substrate is removed, such that only a thin metasurface is left on the transparent substrate.^{10,14}

3.2 Performance of PC metasurface THz detectors

Both designs of the PC metasurface THz detectors are tested for detection of THz pulses using a THz time-domain spectroscopy system. Experimental details can be found in Ref. 10 and 14. A detected waveform of the THz pulse is shown in Figure 4(a) for the detector with the PC resonator network. The dynamic range at the peak of the THz power spectrum exceeds 60 dB. We find that both devices exhibit the highest SNR at relatively low excitation power. In the case of the network metasurface, the highest SNR is reached at 0.1 mW of excitation power. Figure 4(b) illustrates the underlying reasons: the peak photocurrent exhibits saturation already at 0.1 mW, whereas the RMS noise levels for the optical powers below 0.05 mW, indicating that the optimal operation region is between 0.05 and 0.2 mW.

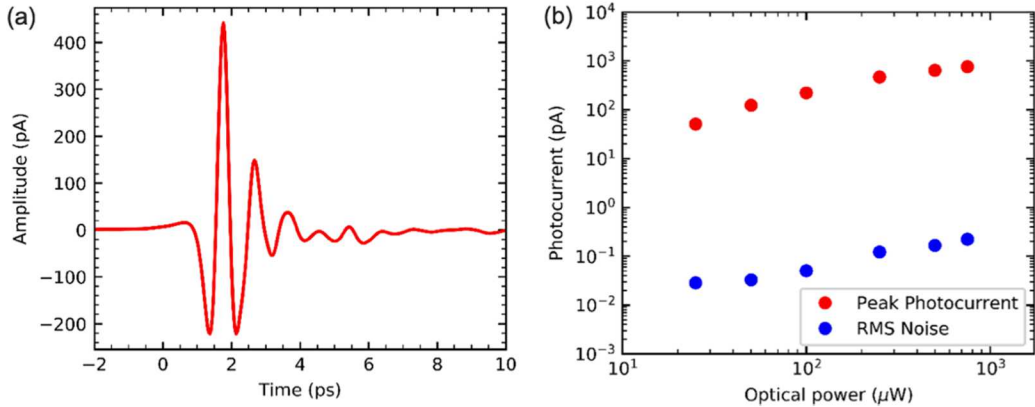


Figure 4. (a) THz pulse waveform measured with the resonator network THz detector using y -polarized optical gating pulses of average power of $100 \mu\text{W}$. (b) Peak THz photocurrent (red) and root-mean squared (RMS) noise (blue) as functions of average power of the optical gate beam [Plots are adapted from Ref. 14].

The required optical power for the optimal performance of this detectors is approximately one order of magnitude lower than what is required for similar THz PC detectors without the metasurface. We attribute this behavior to two factors: first of all, the metasurface enables efficient optical excitation of the PC channel; second, both metasurface structures have higher electrical resistance in comparison to bulk LT GaAs, leading to high dark resistance of the metasurfaces, which in its turn leads to a higher ON/OFF switching contrast. For the resonator network metasurface, we find that the conductivity contrast is higher than 10^7 . The metasurface design therefore allows us to improve two of the key characteristics outlined in Section 1.2.

3.3 Frequency response of PC metasurface THz detectors

The resonant nature of metasurface response leads to prolonged excitation of the photoconductive channel, as the incident photons remain within the metasurface longer than the incident pulse duration. This limits the THz detection bandwidth in general, and below we evaluate the impact of this effect on the overall frequency response of the THz detector.

The THz detector samples the THz field concentrated by the THz antenna in the photoconductive gap and the corresponding time-dependent photocurrent $i(\tau)$ is a cross-correlation function of the time-dependent bias V_{THz} (directly related to the THz field in the gap) and the photo-generated charge carrier density n :

$$i(\tau) = A \int_{-\infty}^{+\infty} V_{\text{THz}}(t) \cdot n(t - \tau) dt. \quad (1)$$

According to the convolution theorem, we can express the Fourier spectrum of the photocurrent $F\{i(t)\}$ as a product of the Fourier transforms of the bias and the charge carrier density function:

$$F\{i(\tau)\} = A \cdot F\{V_{THz}(t)\} \cdot F\{n(-t)\}. \quad (2)$$

The carrier density function $n(t)$ is a convolution of the optical field evolution in the metasurface $I(t)$ and the carrier recombination function $r(t)$, i.e. according to the convolution theorem:

$$F\{n(t)\} = B \cdot F\{I(t)\} \cdot F\{r(t)\}. \quad (3)$$

Therefore, the power spectral density measured in the experiments can be expressed:

$$F\{i(\tau)\} = AB \cdot F\{V_{THz}(t)\} \cdot F\{I(-t)\} \cdot F\{r(-t)\}. \quad (4)$$

Therefore, the prolonged excitation of the PC channel directly affects the spectral response of the THz detector through the multiplication factor $F\{I(t)\}$.

As a practical example we consider the effect of photon trapping in the metasurface on the bandwidth of the metasurface-based THz detector, by assuming that the optical excitation is increased from 70 fs (typical duration of the laser pulse excitation), to 120 fs, as illustrated in Figure 5a. We adjust the amplitude of $I_l(t)$ so that the time-averaged intensity of the optical field in the metasurface for the 120 fs excitation case is 1.4 times higher than that for the 70 fs case. This reflects the fact that optical absorption in the metasurface is 1.4 higher. According to Equation 4, the detected spectral density for the two case differs by the ratio of the Fourier transforms of the optical intensity evolution. This ratio is plotted in Figure 5(b); it shows that the increase in the time that photons remain trapped in the metasurface affect the frequency response of the THz detector. At lower frequencies, it enhances the frequency response; at higher frequencies, however the response becomes lower. The frequency at which the frequency response for the two cases is identical is ~ 3 THz, sufficiently high for typical THz time domain spectroscopy systems.

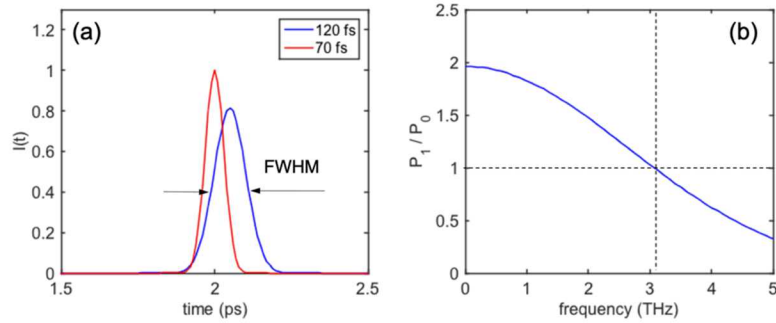


Figure 5. Evaluation of the effect of the optical field evolution in the PC metasurface on the frequency response of the THz detector. (a) Optical field evolution functions $I(t)$ with the intensity FWHM of 70 fs and 120 fs; and (b) the ratio of their Fourier transforms showing the effect of prolonged PC channel excitation on the THz detector bandwidth.

4. CONCLUSIONS

We developed photoconductive THz detectors with integrated perfectly-absorbing photoconductive all-dielectric metasurfaces. The metasurface allows us to improve the efficiency and performance of THz detectors in the frequency range of typical THz time-domain spectroscopy systems (0.1-3.0 THz). We considered two approaches to realize perfect

light absorption in the photoconductive channel without introducing metallic elements. In addition to providing efficient optical absorption, the photoconductive channel based on the resonator network metasurface allows us to engineer desired electrical properties, specifically, fast and efficient conductivity switching with very high contrast. We demonstrate that THz photoconductive detectors with integrated all-dielectric metasurfaces can outperform standard THz detectors based on an unstructured PC channel.

The all-dielectric metasurface approach promises a new generation of sensitive and efficient THz photoconductive detectors. We demonstrate THz pulse detection with SNR of more than six orders of magnitude using an unprecedentedly low level of ultrafast laser excitation of 100 μ W. We attribute the extremely low switching power and excellent noise performance to perfect-absorption properties of the metasurface as well as its nanostructure, which results in extremely high dark resistivity. The photoconductive metasurface is compatible with many practical devices, such as THz emitters, detectors and modulators, and it opens paths for improving their efficiencies.

ACKNOWLEDGEMENTS

This work was supported by the U.S. Department of Energy, Office of Basic Energy Sciences, Division of Materials Sciences and Engineering, and by the EPSRC (EP/L015277/1, EP/P021859/1, EP/L015455/1). Fabrication, optical, and in part THz experiments were performed at the Center for Integrated Nanotechnologies, an Office of Science User Facility operated for the U.S. Department of Energy (DOE) Office of Science. Sandia National Laboratories is a multimission laboratory managed and operated by National Technology and Engineering Solutions of Sandia, LLC., a wholly owned subsidiary of Honeywell International, Inc., for the U.S. Department of Energy's National Nuclear Security Administration under contract DE-NA-0003525. This paper describes objective technical results and analysis. Any subjective views or opinions that might be expressed in the paper do not necessarily represent the views of the U.S. Department of Energy or the United States Government.

REFERENCES

- [1] Yardimci, N. T. and Jarrahi, M. "Nanostructure-Enhanced Photoconductive Terahertz Emission and Detection," *Small* 14 (44), 1802437 (2018).
- [2] Lepeshov, S., Gorodetsky, A., Krasnok, A., Toropov, N., Vartanyan, T. A., Belov, P., Alú, A., Rafailov, and E. U. "Boosting Terahertz Photoconductive Antenna Performance with Optimised Plasmonic Nanostructures," *Sci. Rep.* 8(1), 6624 (2018).
- [3] Heshmat, B., Pahlevaninezhad, H., Pang, Y., Masnadi-Shirazi, M., Burton Lewis, R., Tiedje, T., Gordon, R., and Darcie, T. E. "Nanoplasmonic Terahertz Photoconductive Switch on GaAs," *Nano Lett.* 12(12), 6255–6259 (2012).
- [4] Berry, C. W., Wang, N., Hashemi, M. R., Unlu, M., and Jarrahi, M. "Significant Performance Enhancement in Photoconductive Terahertz Optoelectronics by Incorporating Plasmonic Contact Electrodes," *Nat. Commun.* 4(1), 1622 (2013).
- [5] Jafarlou, S., Neshat, M., and Safavi-Naeini, S. "A Hybrid Analysis Method for Plasmonic Enhanced Terahertz Photomixer Sources," *Opt. Express* 21(9), 11115 (2013).
- [6] Jooshesh, A., Smith, L., Masnadi-Shirazi, M., Bahrami-Yekta, V., Tiedje, T., Darcie, T. E., and Gordon, R. "Nanoplasmonics Enhanced Terahertz Sources," *Opt. Express* 22 (23), 27992 (2014).
- [7] Mitrofanov, O., Brener, I., Luk, T. S., and Reno, J. L., "Photoconductive Terahertz Near-Field Detector with a Hybrid Nanoantenna Array Cavity," *ACS Photonics* 2(12), 1763–1768 (2015).
- [8] Thompson, R. J., Siday, T., Glass, S., Luk, T. S., Reno, J. L., Brener, I., and Mitrofanov, O., "Optically Thin Hybrid Cavity for Terahertz Photo-Conductive Detectors," *Appl. Phys. Lett.* 110 (4), 041105 (2017).
- [9] Castro-Camus, E., and Alfaro, M., "Photoconductive Devices for Terahertz Pulsed Spectroscopy: A Review," *Photonics Res.* 4 (3), A36 (2016).
- [10] Mitrofanov, O., Siday, T., Thompson, R. J., Luk, T. S., Brener, I., and Reno, J. L., "Efficient Photoconductive Terahertz Detector with All-Dielectric Optical Metasurface," *APL Photonics* 3(3), 51703–51703 (2018).
- [11] Ming, X., Liu, X., Sun, L., and Padilla, W. J., "Degenerate Critical Coupling in All-Dielectric Metasurface Absorbers," *Opt. Express* 25(20), 24658 (2017).

- [12] Piper, J. R., Liu, V., and Fan, S., “Total Absorption by Degenerate Critical Coupling,” *Appl. Phys. Lett.* 104 (25), 251110 (2014).
- [13] Cole, M. A., Powell, D. A., and Shadrivov, I. V., “Strong Terahertz Absorption in All-Dielectric Huygens’ Metasurfaces,” *Nanotechnology* 27 (42), 424003 (2016).
- [14] Siday, T., Vabischevich, P.P., Hale, L., Harris, C.T., Luk, T.S., Reno, J.L., Brener, I., and Mitrofanov, O., “Terahertz Detection with Perfectly-Absorbing Metasurface,” *Nano Lett.* 19, 2888-2896 (2019).